Journal of Power Sources 401 (2018) 245–254

Contents lists available at ScienceDirect

Journal of Power Sources

journal homepage: www.elsevier.com/locate/jpowsour

Performance of plug-in hybrid electric vehicle under low temperature condition and economy analysis of battery pre-heating

Tianze Wang[a,b], Xiaogang Wu[a,b], Shaobing Xu[c], Heath Hofmann[d], Jiuyu Du[b], Jianqiu Li[b], Minggao Ouyang[b], Ziyou Song[b,d,*]

[a] College of Electrical and Electronics Engineering, Harbin University of Science and Technology, Harbin, 150080, China
[b] State Key Laboratory of Automotive Safety and Energy, Tsinghua University, Beijing, 100084, PR China
[c] Department of Mechanical Engineering, The University of Michigan, Ann Arbor, MI, 48109, USA
[d] Department of Electric Engineering and Computer Science, The University of Michigan, Ann Arbor, MI, 48109, USA

HIGHLIGHTS

- The performance of the PHEV with a battery pre-heating process is analyzed.
- Battery degradation cost, electricity cost, and fuel cost are considered simultaneously.
- The economy of battery pre-heating powered by engine or grid is analyzed.
- The pre-heating strategy can reduce the operating cost of PHEV by up to 22.3%.

ARTICLE INFO

Keywords:
Plug-in hybrid electric vehicle
Operating cost
Battery pre-heating
Battery degradation
Fuel economy

ABSTRACT

This paper presents a performance analysis of plug-in hybrid electric vehicles (PHEVs) considering battery preheating economy under low temperature conditions. In subzero temperature environments, PHEVs suffer a dramatic loss of all-electric driving range due to the energy and power reduction of $LiFePO_4$ batteries, as well as severe battery degradation due to lithium ion plating. This decreases the battery life time and thus increases the operating cost of the PHEV. A quasi-static model is adopted for the simulated bus, and a battery dynamic degradation model is established based on the Arrhenius degradation theory. The PHEV performance under low-temperature conditions is evaluated considering three factors: fuel cost, electricity cost, and battery degradation cost. In addition, the economics of battery preheating powered by the engine or grid is first investigated in this paper. The charge depleting-charge sustaining energy management strategy and convective heating method are adopted. Simulation results show that the preheating strategy can reduce the PHEV operating cost by up to 22.3% in 40 Harbin driving cycles. The heating process becomes increasingly necessary as the battery price, heating efficiency, and daily recharging time of the PHEV increase as well as the environment temperature decreases.

1. Introduction

Plug-in hybrid electric vehicles (PHEVs) can reduce fuel consumption by downsizing the engine and increasing the electricity utilization. PHEV integrates a large-capacity battery pack, which can be charged from the grid and can handle the daily usage of many car owners using electrical energy only [1,2]. However, PHEVs suffer at low temperatures due to poor battery performance [3,4]. In subzero temperature environments, Li-ion batteries can experience significant capacity loss for several reasons [5–7]: 1) the electrolyte becomes viscous, and even partially solidified, which results in low ionic conductivity; 2) the compatibility between the electrolyte and electrode is deteriorated; 3) the cathode is delithiated and the anode is over-lithiated. The precipitated lithium metal reacts with the electrolyte, and product deposition leads to the thickening of solid electrolyte interface (SEI) film; and 4) the activity of Li^+ in the electrolyte decreases at low temperatures.

Therefore, to avoid battery degradation at low temperatures, one method is to preheat the onboard battery pack before starting the vehicle [8–10]. Ji et al. invented a mutual pulse heating method using a

* Corresponding author. State Key Laboratory of Automotive Safety and Energy, Tsinghua University, Beijing, 100084, PR China.
E-mail addresses: wangtz8255@163.co (T. Wang), ziyou.songthu@gmail.com (Z. Song).

https://doi.org/10.1016/j.jpowsour.2018.08.093
Received 7 May 2018; Received in revised form 13 August 2018; Accepted 30 August 2018
Available online 05 September 2018
0378-7753/

Nomenclature

A	Frontal area
A_h	Ampere-hour throughput
C_{cell}	Capacity of battery cell
c_d	Aerodynamic drag coefficient
c_j	Battery concentration
c_r	Rolling resistance coefficient
c_v	Low heat value of fuel
E_a	Activation energy
h_{bat}	Heat transfer coefficient
I_{bat}	Battery current
J	Total inertia
M_{bat}	Parallel number of battery cell
m_{bat_cell}	Battery cell weight
m_{EGU}	EGU weight
m_p	Passenger weight
m_{veh}	Vehicle body weight
N_{bat}	Series number of battery cell
n	Charge or discharge rate
p_{bat}	Battery price
P_{bat}	Battery power
P_{dem}	Power demand
P_{egu}	EGU power
p_{ele}	Electricity price
p_{fuel}	Fuel price
P_{heat}	Heating power
$P_{preheat}$	Preheating power
Q_{bat}	Capacity of battery pack
Q_{loss}	Battery degradation
R	Gas constants
R_{bat}	Resistance of battery cell
$R_{bat\_cell,ch}$	Charge resistance of battery cell
$R_{bat\_cell,disc}$	Discharge resistance of battery cell
R_w	Wheel radius
SOC_{low}	Low threshold of state of charge
SOC_{high}	High threshold of state of charge
T	Absolute temperature
T_{bat}	Battery temperature
T_{env}	Ambient temperature
T_s	Sampling time
U_{bat}	Battery potential voltage
V_{bat}	Cell voltage
V_{nom}	Nominal voltage of battery cell
ΔA_h	Ah-throughput
η_{DC}	Efficiency of DC/DC converter
η_{EGU_max}	Maximum efficiency of EGU
η_{heat}	Heating efficiency
η_T	Powertrain efficiency
ρ	Air density
$\overline{Q}_{bat}$	Battery heating power
U_{bat}^{avg}	Battery equilibrium potential
ΔH_i	Variation of enthalpy at i-th step
$\overline{H}_j$	Partial molar enthalpy of species j

Acronyms

AER	All electric range
BDC	Battery degradation cost
BPC	Battery preheating cost
CD-CS	Charge depleting-charge sustaining strategy
EC	Electricity cost
ECU	Electric control unit
EMS	Energy management strategy
EGU	Engine and generator unit
FC	Fuel cost
HESS	Hybrid energy storage system
ICE	Internal combustion engine
IHG	Internal heat generation
OCV	Open circuit voltage
PHEV	Plug-in hybrid electric vehicle
PMP	Pontryagin's minimum principle
SEI	Solid electrolyte interface
TCS	Thermostat control strategy

high-efficiency DC/DC converter; the results show that Li-ion batteries can be heated from −20 °C to 20 °C at the expense of only 5% state of charge [8]. Hande et al. developed an internal heating method for EV/HEV batteries using AC currents of varying frequency. The results show that its heating time is shorter and the energy consumption is lower when compared to the low-frequency (60 Hz) heating method [11].

As reported in Ref. [12], the energy management strategy (EMS) significantly affects the vehicle energy efficiency. The EMS of PHEVs can be categorized as “on-line” and “off-line” strategies. The “on-line” strategy, such as the thermostat control strategy (TCS) [13], the charge depleting-charge sustaining (CD-CS) strategy [14–16], the fuzzy logic strategy [17], and the model predictive control strategy [18] can be easily implemented in practical applications. For the off-line EMS, the optimal power allocation can be achieved under a pre-defined driving cycle. For example, Chen et al. [19] used dynamic programming (DP) to optimize energy efficiency of electric vehicle powertrain. Sebastien et al. [20] and Hou et al. [21] used Pontryagin's minimum principle (PMP) to achieve a good balance between fuel consumption and emissions. Qin et al. [22] developed a novel multi-mode hybrid powertrain for tracked vehicles and proposed a novel EMS to obtain near-optimal performance. Wu et al. [23] and Hu et al. [24,25] presented convex optimization for minimizing diesel (electricity) consumption and battery sizes. Song et al. [26] proposed a multi-objective optimization of the hybrid energy storage system (HESS) to minimize the operating cost. Thermal analysis and cost minimization analysis for HESS at subzero temperatures were also presented [27].

On-line strategies can be adopted in real applications; however, in general, they cannot achieve globally optimal results. In contrast, the off-line strategy has satisfactory performance but the computational cost is high. In this paper, the CD-CS, which is a widely-used online strategy for PHEVs, is used.

PHEVs suffer a severe loss of all-electric driving range in subzero temperature environments, and the PHEV operating cost increases due to battery degradation. Therefore, PHEV performance at low temperatures should be investigated and a preheating strategy should be developed in order to improve the PHEV's performance. To the best of our knowledge, this is the first paper focusing on PHEV performance and the necessity of preheating at subzero temperatures. Due to the significant effect of temperature on PHEVs' all-electric driving range and operating cost, this paper aims at exploring the quantitative impact of preheating, a potentially effective solution to the issues arising from low temperatures. Specifically, this paper provides analysis on (1) whether it is cost effective to preheat PHEV batteries at different temperatures, (2) which power source should be selected, i.e., engine or grid, to achieve an effective heating performance, and (3) the sensitivity of the preheating performance to the parameter variation.

This paper focuses on a bus operating in Harbin, China, and presents a method to analyze the operating cost of a PHEV including fuel cost, electricity cost, battery preheating cost, and battery degradation cost. Convection heating is adopted to heat the battery pack. Simulation results show that the heating process becomes increasingly necessary with an increase in all electric range, battery price, and heating

efficiency, as well as a decrease in environment temperature. This paper presents beneficial results about quantifying the benefit of pre-heating process. In addition, the economy analysis related to onboard (i.e., APU) and off board (i.e., charging pile) heating methods are also investigated, and some new insights in terms of the battery pre-heating of PHEV are therefore provided.

This paper is organized as follows. In Section 2, the PHEV model is introduced. In Section 3, the CD-CS EMS incorporating the preheating process is presented. In Section 4, the heating requirement is analyzed from the perspective of operating cost. A discussion is provided in Section 5 and conclusions are drawn in Section 6.

2. PHEV powertrain and battery modeling

In this section, a PHEV model is presented. The studied PHEV has a series powertrain architecture, where the battery pack can be heated through a convective heating device at low temperature conditions, as shown in Fig. 1. The engine is decoupled from the final drive thus it can be controlled at its most efficient operating point. The regenerative braking energy can be recovered by the battery pack, which significantly reduces the CO_2 emissions of a vehicle. The convective heating device, which employs a resistive heater and a fan, is employed in this paper due to its effective and fast heating performance [26]. The heating resistor converts electric power to heat, and the fan creates a convective flow to enhance heat transfer from the heater to the battery cell. For simplicity, battery cells are assumed to have uniform temperature distribution.

2.1. Battery model

2.1.1. The Rint model

Several models have been developed to simulate battery behavior [28–31], such as the equivalent circuit model and the electrochemical model. In this paper the *Rint* model is used, as shown in Fig. 2(a), where U_{bat} is the battery potential and R_{bat} is the resistance of the battery cell [32]. The battery used in the paper is the 3.2 V-60 A h-LFP type battery produced by China Aviation Lithium Battery Co., Ltd (CALB). The battery parameters are measured in the previous experiments and the 10s impedance is used in the battery model. The detailed information about the experiment process is provided in Ref. [26]. The parameters of the $LiFePO_4$ cell are listed in Table 1.

The charge/discharge resistance ($R_{\text{bat\_cell,ch}}/R_{\text{bat\_cell,\ disc}}$) and open circuit voltage (OCV) of the battery cell under different SOCs at 15 °C are measured, as shown in Fig. 2(b). Assuming that the battery pack is grouped by cells through N_{bat} in series and M_{bat} in parallel, the related parameters of the battery pack are given as

$$\begin{cases} R_{\text{bat,ch}} = N_{\text{bat}} R_{\text{bat\_cell,ch}}/M_{\text{bat}} \\ R_{\text{bat,disc}} = N_{\text{bat}} R_{\text{bat\_cell,disc}}/M_{\text{bat}} \\ Q_{\text{bat}} = N_{\text{bat}} M_{\text{bat}} Q_{\text{bat\_cell}} \\ V_{\text{bat}} = N_{\text{bat}} V_{\text{bat\_cell}} \end{cases}, \tag{1}$$

where $R_{\text{bat\_ch}}/R_{\text{bat\_disc}}$ is the charge/discharge resistance of the battery pack, V_{bat} is the battery pack voltage, and $Q_{\text{bat\_cell}}$ and Q_{bat} are capacities of the battery cell and the battery pack respectively.

2.1.2. Battery degradation model

Experts and scholars have made substantial efforts to predict the capacity degradation of batteries in recent years. Liu et al. conducted a series of charge/discharge experiments through constant current-constant voltage mode and used a scanning electron microscope to characterize the structure of the cathode, anode, and separator in Li-ion batteries [33]. Wang et al. [34] designed several charge and discharge experiments in order to calibrate the key parameters in the *Arrhenius* model. The results have shown that battery degradation is related to the charge/discharge rate. In this paper, the semi-empirical model developed in Ref. [27] is adopted:

$$Q_{loss} = Be^{-\left(\frac{E_a+an}{RT}\right)}A_h^x, \tag{2}$$

where E_a and R are the activation energy and gas constant. T and A_h are the absolute temperature and Ampere-hour throughput, n is the charge and discharge rate. B, a, and x are shaping constants. The specific parameters adopted in this paper were calibrated in a previous battery degradation experiment [27]. Eq. (3) is obtained based on the discretization form of Eq. (2).

$$Q_{loss\_k+1} - Q_{loss\_k} = 9.78 \times 10^{-4} e^{-\left(\frac{15162-1516n}{0.849R|285.75-T|+265)}\right)} \Delta A_h Q_{loss\_k}^{-0.1779} \tag{3}$$

where $Q_{\text{loss\_k}}$ and $Q_{\text{loss\_k+1}}$ are the percentages of degenerated battery capacity at time step t_k and t_{k+1}, respectively. ΔA_h is the Ah-throughput from t_k to t_{k+1} calculated by Eq. (4), where Δt is the time period between t_k and t_{k+1}.

$$\Delta A_h = \frac{1}{3600}|I_{bat}|\Delta t \tag{4}$$

To note that the optimal temperature varies depending on the battery type and the load cycle characteristics. For some cases, the optimal temperature of the battery may be higher than 30 °C, in particular if the cycles involve high power charging processes. Therefore, there is limitation of this paper, since we only focus on the specific battery based on [27] where the optimal temperature is about 13 °C. Since the same battery previously studied in Ref. [27] is also used in this paper, the same battery degradation model is employed here.

2.1.3. Battery thermal model

The battery thermal model is important to estimate the battery temperature change at low temperatures, which is necessary for this study. The battery thermal model can be expressed as

$$\begin{aligned} \dot{Q}_{bat} = {} & I_{bat}(U_{bat}^{avg} - V_{bat}) - I_{bat} T_{bat} \frac{\partial U_{bat}^{avg}}{\partial T_{bat}} \\ & - \sum_i \Delta H_i^{avg} r_i - \int \sum_i (\overline{H_j} - \overline{H_j}^{avg}) \frac{\partial c_j}{\partial t} dv, \end{aligned} \tag{5}$$

where $\dot{Q}_{bat}$ is the battery heating power, I_{bat} is the battery current, U_{bat}^{avg} is the battery equilibrium potential (the value with superscript *avg* denotes an average concentration in a certain volume), V_{bat} is the cell voltage, T_{bat} is the battery temperature, ΔH_i is the variation of enthalpy at i-th step. $\overline{H_j}$ is the partial molar enthalpy of species j, c_j is its

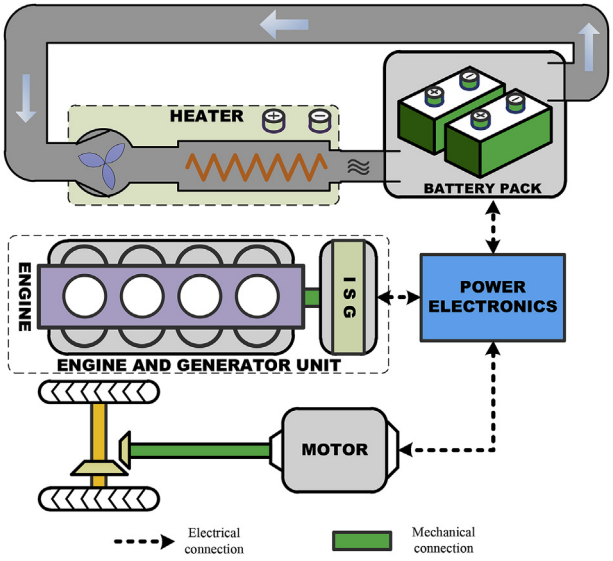

Fig. 1. The configuration of PHEV powertrain incorporating a convective heating function.

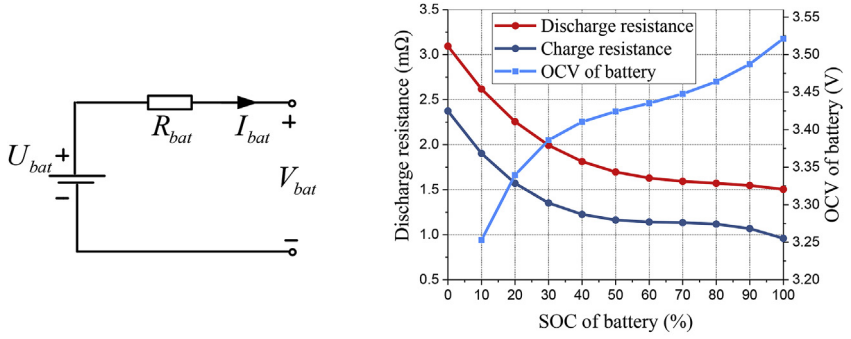

(a) *Rint* model of the $LiFePO_4$ battery. (b) Charge/discharge resistance and OCV of the battery cell.

Fig. 2. The battery model.

Table 1
Parameters of the $LiFePO_4$ battery cell.

Parameter	Value
Nominal voltage, V_{nom} (V)	3.2
Capacity, Q_{bat_cell} (A_h)	60
Battery cell weight, m_{bat_cell} (kg)	2
Max dis/charge current (A)	± 540
Operating temperature window (°C)	−20 to 45

concentration, t is the time, and v is the volume. The first term on the right hand is the heat generated from resistive dissipation, which is also called joule heat. The second term is the reversible entropic heat, or the reaction heat indicating the entropic change during the charge/discharge process. The third term indicates the heat absorbed by any chemical reaction that may occur in the battery. The last term represents the mixed heat absorbed by the temperature gradient inside the battery. It should be noted that compared to the first two terms, the last two terms are very small and therefore ignored. Then thermal model can be simplified as:

$$\dot{Q}_{bat} = I_{bat}(U_{bat}^{avg} - V_{bat}) - I_{bat}T_{bat}\frac{\partial U_{bat}^{avg}}{\partial T_{bat}} \tag{6}$$

Combined with the *Rint* model shown in Fig. 2(a), the joule heat can be calculated. The reaction heat is determined by the battery temperature and the entropic potential ($\partial U_{bat}^{avg} / \partial T_{bat}$). Considering heat dissipation, the complete battery thermal model is described as [26]:

$$N_{bat}M_{bat}C_{cell}\frac{dT_{bat}}{dt} = P_{heat}\eta_{heat} - h_{bat}(T_{bat} - T_{env}) + \dot{Q}_{bat}, \tag{7}$$

where C_{cell} is the thermal capacity of battery cell, P_{heat} is the heat power, h_{bat} is the heat transfer coefficient, η_{heat} is the heating efficiency, and T_{env} is the ambient temperature. The C_{cell} is 2299 J/°C, and h_{bat} is set to 15 W/°C based on experimental results.

There are three factors, which are a) heat-transfer from battery cells to ambient air, b) average battery power efficiency, and c) ambient temperature, to affect the heat management of battery packs. In our previous work, the heat transfer coefficient and the battery power efficiency are considered and analyzed, and it turns out that these two factors do not significantly influence the economy of pre-heating process when compared to the other factors (e.g., ambient temperature) considered in this paper, since the internal heat generation power of battery is much lower than the convective heating power, in addition, only a small power is required to maintain the battery temperature even when the temperature is low [27].

2.2. Engine and generator unit model

The engine and generator unit (EGU) consists of an internal combustion engine (ICE) and an integrated starter generator (ISG) [24,35]. The operation of the ICE and ISG are coupled because they are coaxially connected. It has been shown that keeping the EGU at its most efficient point can achieve the highest energy efficiency, the least amount of carbon emission, and therefore the best fuel economy [21]. As a result, in this paper we assume that the EGU always operates at its most efficient point, where the output power is 42.9 kW with an efficiency of 37.81% [36]. The parameters of the EGU are shown in Table 2.

2.3. Vehicle dynamics model

A static vehicle dynamics model is used to calculate the power demand based on the driving cycle. Detailed information is presented in Ref. [37]. The output power of the driving motor is calculated based on the demand torque and the angular velocity, as shown in Eq. (8), where k equals to 1 or -1 under driving state or braking state respectively, and T_{dem} and ω_{dem} are be calculated by (9). The parameters used in Eq. (9) are listed in Table 3.

$$P_{dem} = T_{dem}\omega_{dem}\eta_T^{-K}, \tag{8}$$

$$\begin{cases} T_{dem} = \left[(m_{bus}gc_r\cos(\theta) + m_{bus}\,a + m_{bus}g\sin(\theta)) + (\frac{Ja_\omega}{R_w} + \frac{1}{2}\rho A c_d v^2)\right]\frac{R_w}{g_{final}} \\ \omega_{dem} = \frac{vg_{final}}{R_w} \\ m_{bus} = m_{veh} + m_p + m_{EGU} + 1.15N_{bat}M_{bat}m_{bat\_cell} \\ a = \frac{dv}{dt};\ a_\omega = \frac{a}{R_w} \end{cases} \tag{9}$$

We point out that the battery resistance used in this paper is measured by using HPPC test, and the battery thermal model is validated by experiments. Due to the space limitations, the entire experimental results cannot be presented in this paper, and the detailed information is provided in Ref. [26]. In addition, the battery degradation model is also verified by the experimental results under different temperatures, as presented in Ref. [27].

3. Energy management strategy considering pre-heating process

The power demand of the bus should be satisfied, and this is one of the basic functions of the vehicle Electronic Control Unit (ECU). The

Table 2
Parameters of the EGU.

Parameters	Value
Maximum power (kW)	55
η_{EGU_max}, maximum efficiency of EGU (%)	37.81
m_{EGU}, EGU mass (kg)	533

Table 3
Basic parameters of the vehicle.

Items	Parameter	Value
Bus	m_{veh}, vehicle body weight (kg)	1.3×10^4
	m_p, passenger weight (kg)	3×10^3
	c_r, rolling resistance coefficient	0.007
	ρ, air density (kg/m^3)	1.18
	J, total inertia (kg·m^2)	143.41
	A, frontal area (m^2)	7.83
	c_d, aerodynamic drag coefficient	0.75
	R_w, wheel radius (m)	0.51
	g_{final}, final gear ratio	6.2
	η_{DC}, power electronics efficiency (%)	90
	η_T, powertrain efficiency (%)	90
Motor	Rated Power (kW)	100
	Peak Power (kW)	180
	Maximum Torque (N·m)	860
	Maximum Speed (r/min)	4500
	Motor voltage (V)	300–450
Battery pack	Capacity (Ah)	120
	Battery pack voltage (V)	280–510
	N_{bat}, series number in battery pack	140
	M_{bat}, parallel number in battery pack	2

Table 4
Setting of threshold [39].

Threshold	Value
SOC_{low}	0.28
SOC_{high}	0.32
T_{bat_low} (°C)	12
T_{bat_high} (°C)	13

relationship of input power and output power can be expressed by Eq. (10), where P_{bat}, P_{EGU}, and P_{dem} are the battery power, EGU power, and the power demand.

$$P_{bat} + P_{EGU} = P_{dem} + P_{heat} \tag{10}$$

Many EMSs have been reported for the power allocation of PHEVs, such as the work of Hou et al. [21] and Murgovski et al. [38]. However, to the best of our knowledge, none of the existing EMSs considers the preheating process. In this paper, the preheating function is integrated in the CD-CS strategy, which is a widely used method for PHEVs. Since the PHEV can be charged by the grid, there are three potential power sources that can be used to preheat the battery, i.e., grid, EGU, and the battery itself. Using the battery to heat itself is a straightforward approach, but it will cause battery SOC reduction as well as degradation. Using the EGU or the grid to heat the battery is therefore preferred. The

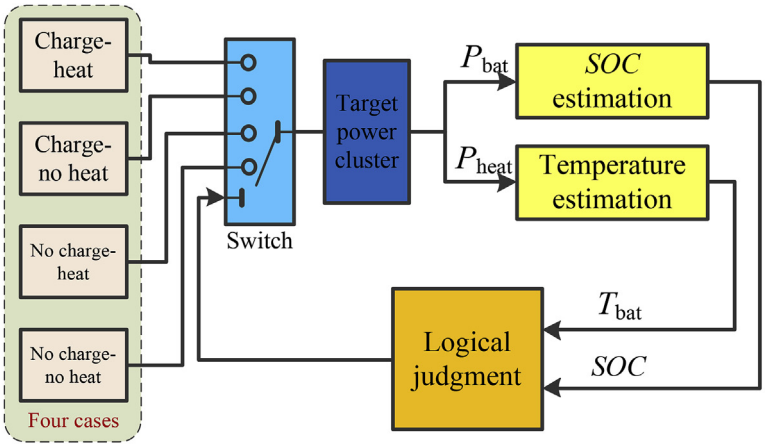

(a) Energy management process.

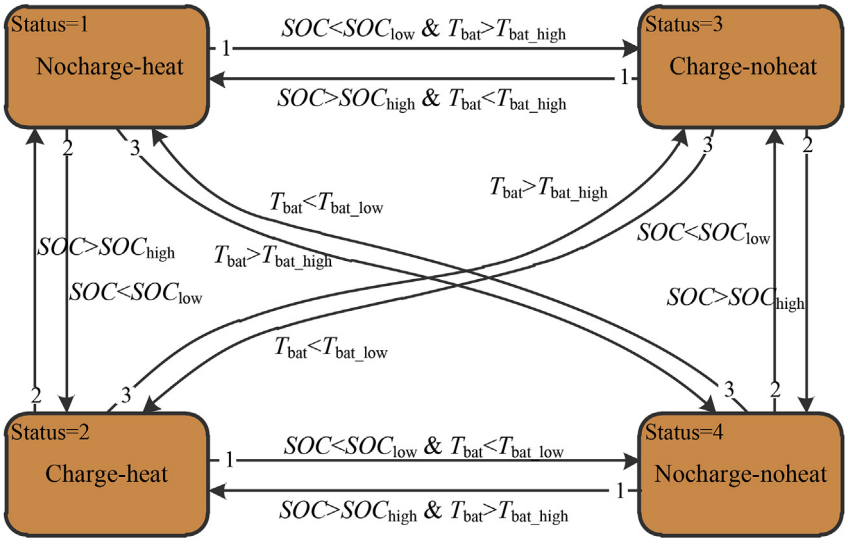

(b) The logic structure of the proposed EMS.

Fig. 3. The CD-CS EMS incorporating preheating function.

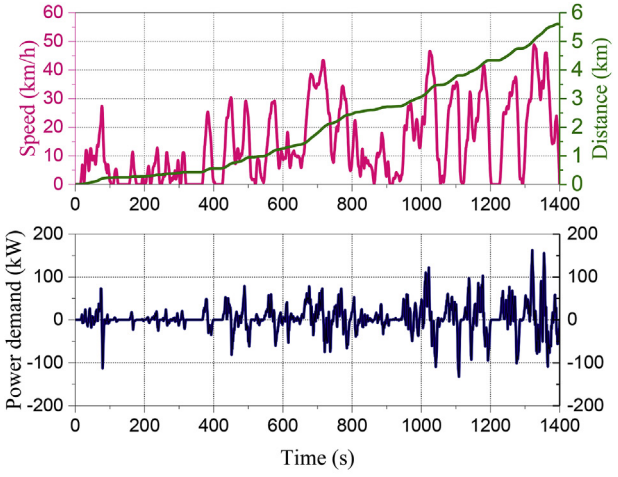

(a) The speed and power profiles of Harbin city driving cycle.

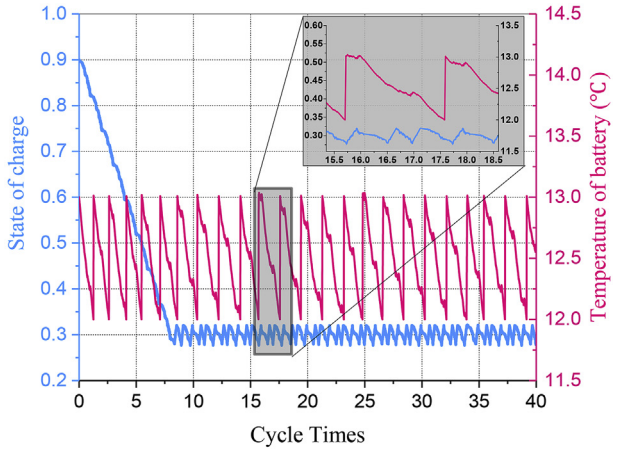

(b) The battery temperature and SOC profiles.

Fig. 4. The Harbin city driving cycle and the simulation result without battery charging process.

EGU can always operate at its highest efficiency point, and the redundant power can be used to heat the battery. When the bus is running, the EGU is the unique power source for supplying the heating power, since the grid is not available. As a result, we mainly investigate the performance of adopting the EGU to heat and insulate the battery pack during the bus is warming up and running. The complete energy management process is depicted in Fig. 3(a).

Given the topology of the series-PHEV, the speed and torque of engine are both decoupled from the wheel. The optimization results of the PHEV operation mode show that the PHEV economy is directly related to the engine working range [15] [22], and it is beneficial to make the engine keep operating in its efficient region. In addition, for the PHEV studied in this paper, our preliminary simulation results show that the engine power can be set to its most efficient value because we can either use the battery to compensate the power (i.e., the difference between the input and output power) or use the additional power to heat the battery. The CD-CS algorithm is proven to be highly effective as compared to ideal fuel economies achievable using dynamic programming approach [16]. The battery is initially further depleted until SOC is lower than a given threshold, and the battery can be charged until the upper threshold of battery SOC is reached [16]. This procedure is repeated over the entire CS phase. In this paper, a similar control algorithm is employed to maintain the battery temperature in its optimal range. Specifically, the battery temperature is controlled between the lower and upper bounds using a bang-bang controller. The specifications about the thresholds for the battery SOC and temperature control are listed in Table 4.

In addition, the four modes illustrated in Fig. 3(a), i.e., charge-heat mode, charge-no heat mode, no charge-heat mode, and no charge-no heat mode, are used to characterize different power allocation scenarios. For example, the charge-no heat means that the battery needs to be charged but the heating process is not applied. Further, we assume that all the energy of the regenerative braking process can be recovered by the battery. The state flow is used to switch between four cases, as shown in Fig. 3(b). When the battery SOC and temperature meet the corresponding conditions, it will jump to the adjacent state. The numbers on the lines indicate the order in which the signals are retrieved. The thresholds mentioned in Fig. 3(b) are specified in Table 4. According to the previous research [27], the adopted LFP battery has the smallest decay at 12.75 °C, hence the maximum operating temperature of the battery pack is set to 13 °C. The EGU is set to control the battery temperature within the range from 12 °C to 13 °C when the bus is running.

The heating power includes two parts, i.e., the preheating power P_{preheat} before bus running and the maintenance power to keep the battery temperature within the appropriate range. The second power is provided by the EGU, as previously mentioned. The preheating power can be provided by either the EGU or the grid. Generally, the bus can be charged by the grid during the night, and the preheating can be conducted simultaneously. Different power sources will result in different preheating costs, which will be quantitatively analyzed in this paper. The Harbin city driving cycle is adopted to test the PHEV, as shown in Fig. 4(a). The distance of one Harbin driving cycle is 5.6 km, and 40 driving cycles (224 km) are used to represent the bus daily driving scenario.

The basic and general scenario considered here is that the battery is preheated from the environment temperature of −20 °C to the optimal temperature of 13 °C (either by the EGU or the grid) and there is no charging opportunity during the daily trip. As shown in Fig. 4(b), the battery SOC and temperature profiles during the daily trip can be obtained based on the PHEV model. It can be seen that the CD stage ends after about 8 driving cycles and then the vehicle enters the CS stage. The battery temperature is maintained within 12°C–13 °C during the entire day. When the ambient temperature is −20 °C and the heating efficiency is supposed to 0.7, the battery temperature and degradation curves are compared with those without the battery heating process, as shown in Fig. 5(a). It can be seen that the temperature of the non-heating case increases to −9 °C after a daily trip due to the battery internal heat generation (IHG). When compared to the non-heating case, the battery degradation is reduced from 1.647×10^{-4} to 0.336×10^{-4} (the battery capacity is normalized to 1) by incorporating the battery heating process, and a significant reduction in the battery replacement cost can be therefore achieved.

To further analyze the system operating costs, the prices of fuel and electricity are listed in Table 5. The current LFP battery price is about 300 $/kW·h [40]. The efficiency of the convective heating process is around 70% [8]. We assume that the battery needs to be replaced when its capacity reduces to 80% of the initial value. The battery is heated form −20 °C to 13 °C by the EGU. The operating cost consists of four costs, which are the FC, EC, BDC and BPC. These costs can be calculated by Eq. (11). The first three costs (FC, EC, BDC) accumulate over entire day, while the BPC, which is equivalent to the fuel cost for heating the battery from the ambient temperature to the suitable temperature, only accumulates in the preheating process. Since in the first case, the battery is preheated by the EGU, and the BPC is calculated by using the EGU heating power and the fuel price. When the battery is preheated by the grid, the BPC can be calculated by substituting the grid heating power and the electricity price. The four costs are shown in Fig. 5(b) and 5(f), where T_s is the sampling time.

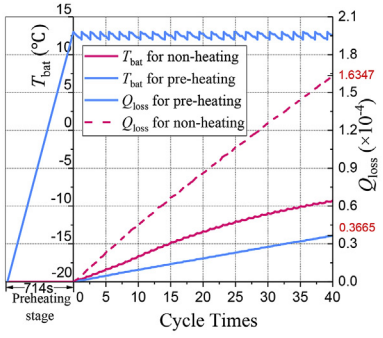

(a)The battery temperature and degradation curves.

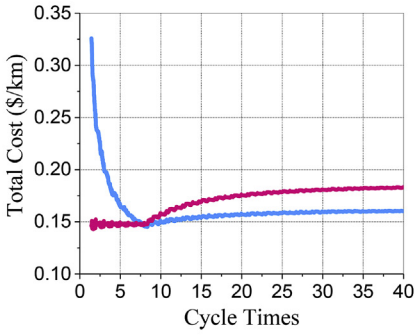

(b)The total operating cost.

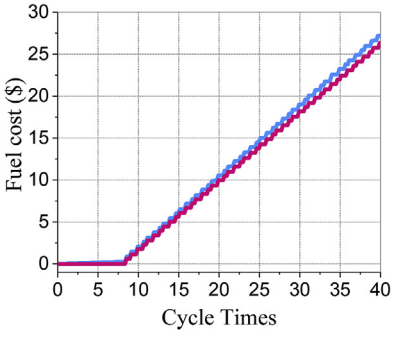

(c)The fuel cost.

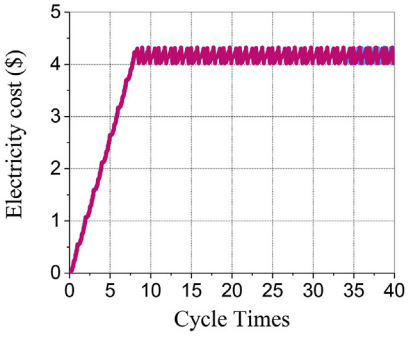

(d)The electricity cost.

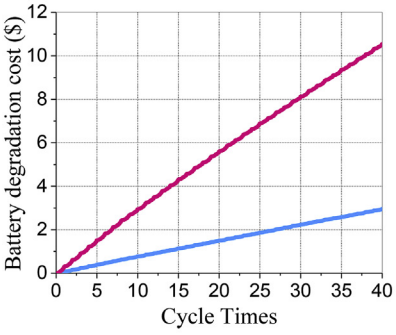

(e)The battery degradation cost.

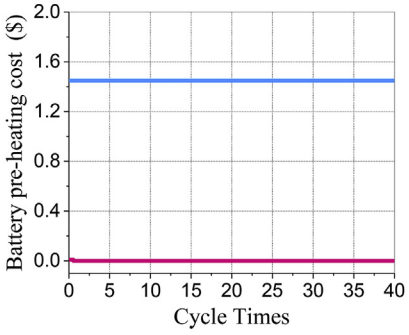

(f)The battery preheating cost.

Fig. 5. The battery pack state change (temperature and Qloss) and operating cost under non-recharging opportunity (▭: operating costs with preheating; ▭: operating costs without preheating).

$$\begin{cases} FC = \sum_k \frac{P_{EGU}(k) p_{fuel} T_s}{\eta_{EGU\_max} c_v} \\ EC = \sum_k \frac{P_b(k) P_{ele} T_s}{3.6 \times 10^6} \\ BDC = \sum_k \frac{Q_{loss\_k} p_{bat}}{0.2} \frac{N_{bat} M_{bat} Q_{bat\_cell} V_{nom}}{1000} \\ BPC = \sum_{T_{bat}=-20°C}^{13°C} \frac{P_{EGU}(T_{bat}) p_{fuel} T_s}{\eta_{EGU\_max} c_v} \end{cases} \quad (11)$$

Table 5
Reference prices and values.

Item	Value
Battery price p_{bat} ($/kW·h)	300 [40]
Electricity price p_{ele} ($/kW·h)	0.129 [41]
Fuel price p_{fuel} ($/L)	0.75 [42]
Heat efficiency η_{heat}	0.7 [8]
Low heat value c_v (J/L)	3.8×10^7
Environment temperature T_{env} (°C)	−20
Maximum efficiency of EGU η_{EGU_max} (%)	42.9

In Fig. 5(c), the FC with the battery heating process is 3.3% higher than that without heating process because the EGU supplies extra power to maintain the battery temperature. However, the BDC can be significantly reduced and the total operating cost can be therefore reduced by 11.1%, as shown in Fig. 5(b). The difference of BDC during one daily trip is 7.55 $, which is a 72.0% saving. Therefore, although the battery heating process will increase the fuel cost, it can significantly reduce overall operating cost and therefore bring the significant benefit for PHEV owners. The effectiveness of the battery heating process is preliminarily verified by above simulation results. In addition, the benefit can be further increased if the preheating process can be conducted by the grid, since electricity is much cheaper than fuel. Different cases will be analyzed and compared in the next section to verify the effectiveness of the battery heating process.

4. Battery heating analysis under different conditions

In this section the battery heating necessity is analyzed under different conditions. In general, bus stations are equipped with chargers. The buses frequently commute between the bus stations. It is possible to start recharging when the bus enters the bus terminal after passing through 20 driving cycles (about 110 km) or after 13 driving cycles (about 75 km). It is necessary to investigate how much mileage is appropriate between charges during the daily trip. The influence of different charging times on the operating cost should be considered. Therefore, two recharging scenarios (recharging once daily, recharging twice daily) are considered to analyze the preheating performance and the PHEV fuel economy. In addition, a parameter sensitivity analysis considering the battery price p_{bat} and environment temperature T_{env} is also presented due to their significant impacts on the result.

The battery SOC and the temperature curves corresponding to the

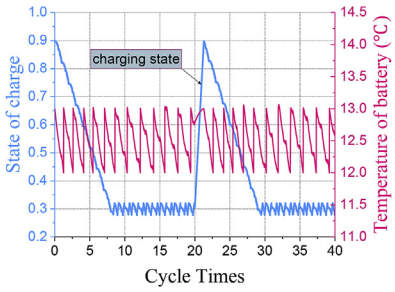

(a)The battery SOC and temperature curves.

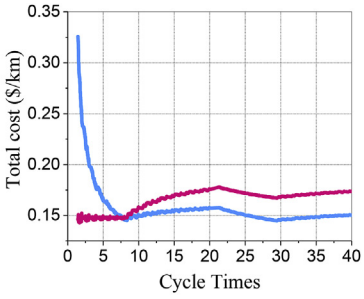

(b)The total cost.

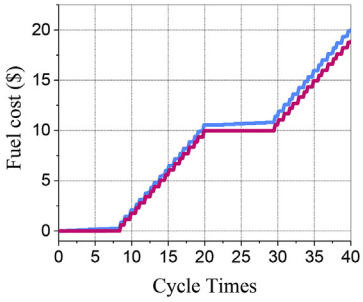

(c)The fuel cost.

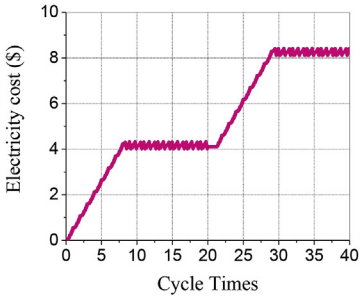

(d)The electricity cost.

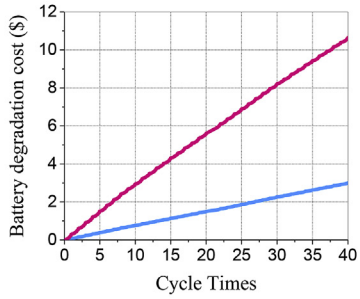

(e)The battery degradation cost.

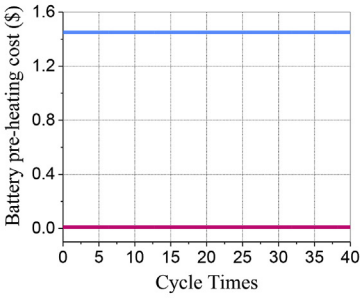

(f)The battery preheating cost.

Fig. 6. The battery pack state change (SOC and temperature) and the operating cost with one recharging opportunity (▭: operating costs with preheating; ▭: operating costs without preheating).

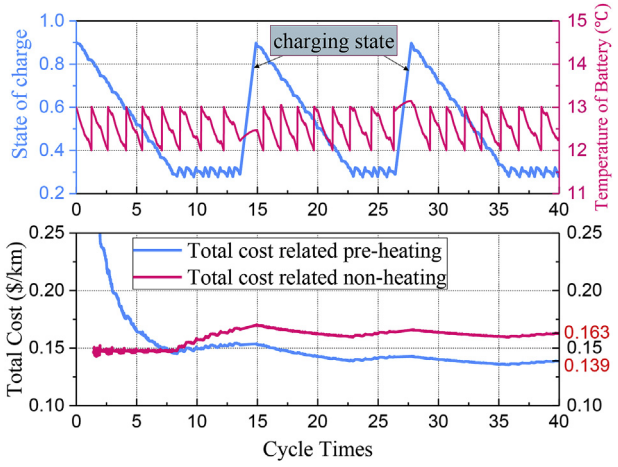

Fig. 7. Simulation results with two recharging opportunities daily.

once-a-day recharging case are shown in Fig. 6(a). After 20 driving cycles, the bus enters the charging station and the battery is recharged at a 2C rate. The operating costs with and without the battery heating process are compared and shown in Fig. 6(b) and 6(f). The FC under the battery heating condition is slightly higher than that under the no heating condition because the battery temperature maintaining needs energy from the EGU. In addition, the BPC is always the additional cost for the battery heating process. In the first 6 driving cycles, the operating cost with the heating strategy is higher than the one without the heating strategy due to the preheating cost. However, after that, the reduction in BDC gradually compensates the negative consequence. By incorporating the heating process, the total cost is reduced by 13.8% (from 0.174 $/km to 0.150 $/km). It can also be found that the recharging process can reduce the PHEV operating cost because more electricity can be used to substitute the fuel. In addition, the battery heating process becomes more important when the recharging opportunity exists because the battery is used more frequently.

The battery SOC, temperature, and operating cost with double recharging opportunities daily are shown in Fig. 7. Under the battery heating condition, the total operating cost can be reduced from 0.150 $/km to 0.139 $/km with an additional recharging opportunity, as shown in Fig. 5(b) and Fig. 6(b). Moreover, it can be seen that the benefit from the battery preheating process also increases with the increasing number of recharge.

The simulation results in this section further verify the effectiveness of the battery heating process when the ambient temperature is low. In addition, the battery heating necessity is enhanced when the PHEV has the recharging opportunity during the daily trip.

Table 6
Total cost under different p_{bat}, T_{env} and with various recharging opportunities.

Recharge time T_{env}		No recharge opportunity		
		−20 °C	−10 °C	0 °C
Battery price, p_{bat}	150 $/kW·h	0.154/0.159 3.2%	0.151/0.156 3.0%	0.145/0.152 2.0%
	300 $/kW·h	0.160/0.183 12.41%	0.156/0.175 10.43%	0.154/0.167 7.78%
	450 $/kW·h	0.167/0.206 19.19%	0.163/0.194 15.89%	0.161/0.183 12.04%
Recharge time T_{env}		Single recharge opportunity		
		−20 °C	−10 °C	0 °C
Battery price, p_{bat}	150 $/kW·h	0.144/0.150 3.8%	0.139/0.144 3.6%	0.135/0.140 3.4%
	300 $/kW·h	0.150/0.174 13.8%	0.146/0.165 11.5%	0.141/0.157 10.2%
	450 $/kW·h	0.157/0.198 20.7%	0.153/0.185 17.3%	0.148/0.173 14.5%
Recharge time T_{env}		Double recharge opportunities		
		−20 °C	−10 °C	0 °C
Battery price, p_{bat}	150 $/kW·h	0.132/0.137 4.2%	0.127/0.132 4.0%	0.122/0.127 3.7%
	300 $/kW·h	0.139/0.163 14.7%	0.134/0.154 13.0%	0.129/0.146 11.6%
	450 $/kW·h	0.146/0.188 22.3%	0.141/0.175 19.4%	0.137/0.163 16.0%

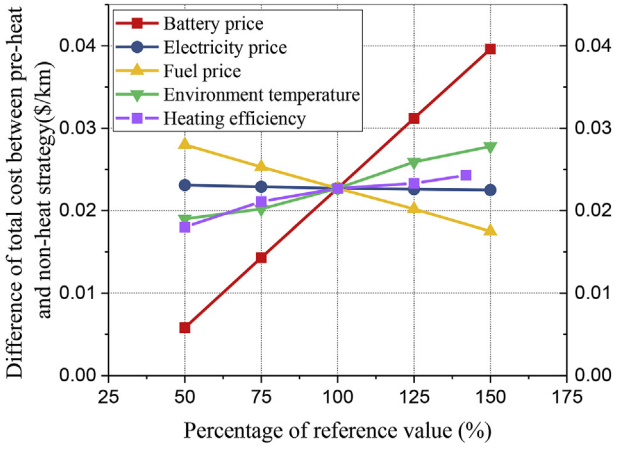

Fig. 8. Parameter sensitivity analysis for the no recharging case.

Table 7
Average monthly temperature and operating cost in Harbin.

Month	Jan	Feb	Mar	Nov	Dec
Average Temp (°C)	−18.3	−13.6	−3.4	−5.3	−14.8
Total operating cost for preheating strategy	978.0	964.3	933.0	938.1	968.1
Total operating cost for non-heating strategy	1125.0	1097.7	1044.3	1053.6	1104.3

5. Discussion

For now, the price of Lithium batteries varies in the range of 200–400 $/kW·h [43,44]. To be specific, the cost of battery packs used by market-leading EV manufacturers have declined by 8% annually between 2007 and 2014 [43]. Analysts from McKinsey stated in 2012 that $200/kW·h could be reached in 2020, and $160/kW·h could be reached in 2025 [44]. The Lithium ion battery price has continuously and significantly decreased in China in recent years. Therefore, three prices, (150 $/kW·h, 300 $/kW·h, and 450 $/kW·h) are considered in this paper to analyze the influence of battery price on the simulation result. Three ambient temperatures (i.e., −20 °C, −10 °C, 0 °C), are also considered for the comparison study. The PHEV operating costs with and without the battery heating process are compared for different scenarios, as shown in Table 6. It can be seen that the heating strategy is beneficial for all cases. The heating process becomes increasingly necessary as the battery price, heating efficiency, and number of recharges of the PHEV increase as well as the environment temperature decreases. When the battery price is as low as 150 $/kW·h and the ambient temperature is 0 °C, the operating cost still has a reduction of 2.7% when incorporating the battery heating process. Therefore, it is always beneficial to heat the battery under sub-zero temperature conditions. The benefit decreases as T_{env} increases because the difference in the battery degradation of the heating and non-heating cases becomes less obvious. The BDC is proportional to the battery price, thus the benefit of battery heating reduces when the battery price decreases. It is possible that the battery heating will become unnecessary when the ambient temperature further increases or the battery price further decreases.

A further sensitivity analysis is conducted for the case without recharging opportunity, as shown in Fig. 8. It can be seen that the preheating benefit decreases with the increase of fuel price because the FC for maintaining the battery temperature increases. The total cost difference varies slightly with respect to the electricity price because the EC of different cases are almost the same. It is clear that the preheating performance can be improved as the heating efficiency increases.

Due to space limitations, the analysis of battery pre-heating by using the grid cannot be extended. But we point out that the pre-heating via the grid can further increase the benefit because the electricity price is much lower than the fuel price. For example, when the battery price is 450 $/kW·h and the temperature is −20 °C, the PHEV operating cost decreases from 0.146 $/km to 0.143 $/km when substituting the grid for pre-heating the battery. Therefore, when compared with 0.188 $/km under no recharge, benefits are further improved. When the battery price is 150 $/kW·h and the temperature is 0 °C, the PHEV operating cost decreases from 0.145 $/km to 0.141 $/km when substituting the grid for pre-heating the battery. Therefore, compared with 0.152 $/km under no recharge, benefits are also further improved.

In order to show the benefit of preheating strategy in practical applications, a case study about operating a bus in Harbin, China is presented. There are five months in Harbin with low temperatures, as listed in Table 7 [45]. In November, December, January, February, and March, the temperature drops under 0 °C, and battery heating should be considered based on above analysis. It is assumed that the bus runs 40 Harbin driving cycles (about 224 km) daily. The total operating costs of these five months with one recharging opportunity daily are shown in Table 7. The battery heating strategy saves 643.4 $ in total when compared to the non-heating strategy. In other words, the PHEV can save about 13% of operating costs if the preheating strategy is applied in Harbin.

Based on the simulation results and analysis above, several remarks are provided as follows:

Remark 1. The battery heating process is beneficial under sub-zero temperatures for all battery prices considered in this paper. For a city like Harbin, China, the battery pre-heating is highly recommended in winter to reduce the operating cost, especially the battery degradation cost.

Remark 2. For PHEVs, the recharging opportunity among different driving tasks can significantly reduce the fuel cost. In addition, the reduction of the battery degradation cost via battery pre-heating process can be further increased by the increasing recharging opportunity.

Remark 3. The heating process becomes increasingly necessary as the battery price, heating efficiency, and daily recharging time of the PHEV increase and the environment temperature decreases.

Remark 4. The analysis in this paper adopts the EGU for battery pre-heating, which verifies the effectiveness of the proposed heating strategy. We point out that the grid is preferred as a power source to pre-heat the battery because the electricity is much cheaper than the fuel, which will further improve the battery pre-heating performance.

The convective heating approach is adopted in this paper, and the heating power is around 40 kW, which is relatively high. When the convective heating method is used, it is possible to cause severe cell-to-cell variation in temperature, especially for a large battery pack. Actually, there are other heating methods capable of heating the battery fast and avoiding cell-to-cell temperature variation. For example, the mutual pulse heating [8] and the internal heating [46] approaches can be employed when the heating power is high. Especially, the internal heating approach can raise the battery temperature by 20° in 20 s without any cell-to-cell temperature variation [46]. In practical applications, the heating method should be carefully selected considering the feasibility, the capital cost, and the heating power. This manuscript mainly focuses on the economy analysis, therefore the specific heating method does not influence the results, since the heating efficiency is well considered.

6. Conclusions

This paper analyzes the heating requirements of PHEVs at subzero temperatures. A preheating power management strategy is proposed. The fuel cost, electricity cost, battery degradation cost, and battery preheating cost are considered in the operating cost. The battery price, fuel price, number of daily recharges, and the ambient temperature significantly influence the benefit of the battery preheating process. When the battery price drops to 150 $/kW·h, the preheating still offers about a 2.5% reduction in operating cost when the ambient temperature is 0 °C and no recharging opportunity is available. When the battery price is 450 $/kW·h and the ambient temperature is −20 °C, the operating cost reduction by the heating process is 22.3% with two daily recharging opportunities. A case study for Harbin, China is also conducted, and it shows that there are five months that require the battery heating process in Harbin, and the PHEV can save 643.4 $ totally.

Acknowledgement

This research is supported by Ministry of Education of the People's Republic of China and National Science Foundation of US under Grand No. CNS 1329539.

References

[1] S. Bashash, S.J. Moura, J.C. Forman, H.K. Fathy, Plug-in hybrid electric vehicle charge pattern optimization for energy cost and battery longevity, J. Power Sources 196 (2011) 541–549.
[2] J. Peng, H. He, R. Xiong, Rule based energy management strategy for a series-parallel plug-in hybrid electric bus optimized by dynamic programming, Appl. Energ. 185 (2017) 1633–1643.
[3] Y. Zheng, Y. He, K. Qian, D. Liu, Q. Lu, B. Li, X. Wang, J. Li, F. Kang, Influence of charge rate on the cycling degradation of LiFePO4/mesocarbon microbead batteries under low temperature, Ionics 23 (2017) 1967–1978.
[4] X. Hu, S. Li, H. Peng, A comparative study of equivalent circuit models for Li-ion batteries, J. Power Sources 198 (2012) 359–367.
[5] M. Petzl, M. Kasper, M.A. Danzer, Lithium plating in a commercial lithium-ion battery – a low-temperature aging study, J. Power Sources 275 (2015) 799–807.
[6] V. Agubra, J. Fergus, Lithium ion battery anode aging mechanisms, Materials 6 (2013) 1310–1325.
[7] M. Petzl, M. Kasper, M.A. Danzer, Lithium plating in a commercial lithium-ion battery – a low-temperature aging study, J. Power Sources 275 (2015) 799–807.
[8] Y. Ji, C.Y. Wang, Heating strategies for Li-ion batteries operated from subzero temperatures, Electrochim. Acta 107 (2013) 664–674.
[9] C. Zhu, X. Li, L. Song, L. Xiang, Development of a Theoretically Based thermal Model for Lithium Ion Battery Pack.
[10] N. Damay, C. Forgez, M. Bichat, G. Friedrich, A. Ospina, Thermal Modeling and Experimental Validation of a Large Prismatic Li-ion Battery, IEEE Industrial Electronics Society, 2013, pp. 4694–4699.
[11] T.A. Stuart, A. Hande, HEV battery heating using AC currents, J. Power Sources 129 (2004) 368–378.
[12] F.R. Salmasi, Control strategies for hybrid electric vehicles: evolution, classification, comparison, and future trends, IEEE T Veh Technol 56 (2007) 2393–2404.
[13] S.G. Wirasingha, A. Emadi, Classification and review of control strategies for plug-in hybrid electric vehicles, IEEE Vehicle Power and Propulsion Conference, 2009, pp. 805–812.
[14] Z. Zhiguang, C. Mi, Power management of PHEV using quadratic programming, Int. J. Electr. Hybrid Veh. (IJEHV) 3 (2011) 246–258.
[15] H. Son, H. Kim, S. Hwang, H. Kim, E. Sciubba, Development of an advanced rule-based control strategy for a PHEV using machine learning, Energies 89 (2018).
[16] M. Sorrentino, C. Pianese, M. Maiorino, An integrated mathematical tool aimed at developing highly performing and cost-effective fuel cell hybrid vehicles, J. Power Sources 221 (2013) 308–317.
[17] F. Jin, M. Wang, C. Hu, A fuzzy logic based power management strategy for hybrid energy storage system in hybrid electric vehicles considering battery degradation, 2016 IEEE Transportation Electrification Conference and EXPO, ITEC, 2016.
[18] Z. Song, H. Hofmann, J. Li, J. Hou, X. Han, M. Ouyang, Energy management strategies comparison for electric vehicles with hybrid energy storage system, Appl. Energ. 134 (2014) 321–331.
[19] J. Du, J. Chen, Z. Song, M. Gao, M. Ouyang, Design method of a power management strategy for variable battery capacities range-extended electric vehicles to improve energy efficiency and cost-effectiveness, Energy 121 (2017) 32–42.
[20] S. Delprat, J. Lauber, T.M. Guerra, J. Rimaux, Control of a parallel hybrid powertrain: optimal control, IEEE T Veh Technol. 53 (2004) 872–881.
[21] C. Hou, M. Ouyang, L. Xu, H. Wang, Approximate Pontryagin's minimum principle applied to the energy management of plug-in hybrid electric vehicles, Appl. Energ. 115 (2014) 174–189.
[22] Z. Qin, Y. Luo, W. Zhuang, Z. Pan, K. Li, H. Peng, Simultaneous optimization of topology, control and size for multi-mode hybrid tracked vehicles, Appl. Energ. 212 (2018) 1627–1641.
[23] X. Wu, T. Wang, Optimization of battery capacity decay for semi-active hybrid energy storage system equipped on electric city bus, Energies 10 (2017).
[24] X. Hu, N. Murgovski, L. Johannesson, B. Egardt, Energy efficiency analysis of a series plug-in hybrid electric bus with different energy management strategies and battery sizes, Appl. Energ. 111 (2013) 1001–1009.
[25] Y. Yang, X. Hu, H. Pei, Z. Peng, Comparison of power-split and parallel hybrid powertrain architectures with a single electric machine: dynamic programming approach, Appl. Energ. 168 (2016) 683–690.
[26] Z. Song, J. Li, X. Han, L. Xu, L. Lu, M. Ouyang, H. Hofmann, Multi-objective optimization of a semi-active battery/supercapacitor energy storage system for electric vehicles, Appl. Energ. 135 (2014) 212–224.
[27] Z. Song, H. Hofmann, J. Li, J. Hou, X. Zhang, M. Ouyang, The optimization of a hybrid energy storage system at subzero temperatures: energy management strategy design and battery heating requirement analysis, Appl. Energ. 159 (2015) 576–588.
[28] F. Sun, R. Xiong, H. He, A systematic state-of-charge estimation framework for multi-cell battery pack in electric vehicles using bias correction technique, Appl. Energ. 162 (2016) 1399–1409.
[29] M. Ceraolo, New dynamical models of lead-acid batteries, IEEE T Power Syst. 15 (2000) 1184–1190.
[30] X. Hu, S. Li, H. Peng, A comparative study of equivalent circuit models for Li-ion batteries, J. Power Sources 198 (2012) 359–367.
[31] X. Wu, W. Shi, J. Du, Multi-objective optimal charging method for lithium-ion batteries, Energies 10 (2017).
[32] S.X. Chen, H.B. Gooi, N. Xia, M.Q. Wang, Modelling of lithium-ion battery for online energy management systems, IET Electr. Syst. Transp. 2 (2012) 202–210.
[33] W. Liu, B. Zhou, X. Wang, J. Gao, X. Liu, Capacity fading of 18650 Li-ion cells with cycling, Chin. J. Power Sources 36 (2012) 306–309.
[34] J. Wang, P. Liu, J. Hicks-Garner, E. Sherman, S. Soukiazian, M. Verbrugge, H. Tataria, J. Musser, P. Finamore, Cycle-life model for graphite-LiFePO(4) cells, J. Power Sources 196 (2011) 3942–3948.
[35] N. Murgovski, L. Johannesson, J. Sjoberg, B. Egardt, Component sizing of a plug-in hybrid electric powertrain via convex optimization, Mechatronics 22 (2012) 106–120.
[36] X. Hu, N. Murgovski, L. Johannesson, B. Egardt, Energy efficiency analysis of a series plug-in hybrid electric bus with different energy management strategies and battery sizes, Appl. Energ. 111 (2013) 1001–1009.
[37] X. Wu, T. Wang, Optimization of battery capacity decay for semi-active hybrid energy storage system equipped on electric city bus, Energies 10 (2017).
[38] N. Murgovski, L. Johannesson, J. Sjoberg, B. Egardt, Component sizing of a plug-in hybrid electric powertrain via convex optimization, Mechatronics 22 (2012) 106–120.
[39] S.G. Wirasingha, A. Emadi, I.V.T. Society, Classification and review of control strategies for plug-in hybrid electric vehicles, IEEE T Veh Technol. 60 (2011) 111–122.
[40] A.P.P. Corp, Batteryspace, (2017).
[41] EIA - Electricity Data, 2017.
[42] Gasoline and Diesel Fuel Update, Energy Information Administration, 2017.
[43] B. Nykvist, M. Nilsson, Rapidly falling costs of battery packs for electric vehicles, Nat. Clim. Change 5 (2015) 329–332.
[44] R. Hensley, J. Newman, M. Rogers, Battery Technology Charges Ahead, (2017).
[45] Analysis of Climate Background in Harbin, (2017).
[46] C. Wang, et al., Lithium-ion battery structure that self-heats at low temperatures, Nature 529 (2016) p. 515 EP.